Journal of Chemistry and Technologies, 2021, *29*(4), 485-494

Journal of Chemistry and Technologies

pISSN 2663-2934 (Print), ISSN 2663-2942 (Online).

journal homepage: http://chemistry.dnu.dp.ua

UDC 541.123.3

PHASE RELATION STUDIES IN THE La_2O_3–Lu_2O_3–Yb_2O_3 SYSTEM AT 1500 °C

Olga V. Chudinovych[1,2], Olexandr I. Bykov[1], Anatoly V. Samelyuk[1]

[1] Frantsevich Institute for Problems in Materials Science NAS of Ukraine, Kiev

[2] National Technical University of Ukraine «Igor Sikorsky Kyiv Polytechnic Institute», Kiev

Received 15 August 2021; accepted 9 November 2021; available online 27 January 2022

Abstract

The phase relation in the La_2O_3–Lu_2O_3–Yb_2O_3 ternary system at 1500 °C were studied by X-ray diffraction (XRD) and scanning electron microscopy in the overall concentration range. The test samples of different compositions have been prepared from nitrate acid solutions by evaporation, drying, and calcinations at 800 °C. To study phase relationships at 1500 °C the as-repared samples were thermally treated in two stages: at 1100 °C and then at 1500 °C (for 70 h in air). The phase composition of the test samples studied by X-ray diffraction (XRD, DRON-3), microstructural phase and electron microprobe X-ray (Superprobe-733, JEOL, Japan, Palo Alto, CA) analyses. Solid solutions based on various polymorphic forms of original oxides and ordered LaLuO3 (LaYbO3) phases were detected in the system. No new phases were found in the system. The isothermal section of the phase diagram for the La_2O_3–Lu_2O_3–Yb_2O_3 system has been developed. It was established that in the ternary La_2O_3–Lu_2O_3–Yb_2O_3 system there exist fields of solid solutions based on hexagonal (A) modification of La_2O_3, cubic (C) modification of Y_2O_3 and Lu_2O_3, as well as perovskite-type ordered phases of orthorhombic symmetry $LaLuO_3$ and $LaYbO_3$ (R). The refined lattice parameters of the unit cells for solid solutions and microstructures of the definite field of compositions for the systems solid were determined. The La_2O_3–Lu_2O_3–Yb_2O_3 system forms an infinite series of solid solutions based on the perovskite-type phase. The maximum solubility of Lu_2O_3 in the R-phase is ~6 mol. % along section Lu_2O_3 –(50 mol. % La_2O_3 – 50 mol. % Yb_2O_3). The region of homogeneity of the R-phase extends from 46 to 56 mol. % La_2O_3 in the cross section La_2O_3–(50 mol.% Lu_2O_3–50 mol.% Yb_2O_3).

Keywords: phase equilibria; Lanthana; Lutetia; Ytterbia; lattice parameters

ВЗАЄМОДІЯ ОКСИДІВ ЛАНТАНУ, ЛЮТЕЦІЮ ТА ІТЕРБІЮ ЗА ТЕМПЕРАТУРИ 1500 °C

Ольга В. Чудінович[1,2], Олександр І. Биков[1], Анатолій В. Самелюк[1]

[1]Інститут проблем матеріалознавства ім. І.М. Францевича НАН України, м. Київ

[2]Національний технічний університет України "Київський політехнічний інститут імені Ігоря Сікорського", м. Київ

Анотація

Фазові рівноваги у потрійній системі La_2O_3–Lu_2O_3–Yb_2O_3 за 1500 °C досліджено за допомогою рентгенофазового аналізу (РФА) та скануючої електронної мікроскопії у всьому інтервалі концентрацій. Досліджувані зразки різного складу готували з розчинів нітратів шляхом випарювання, сушіння та прожарювання при 800 °C. Для вивчення фазових рівноваг за 1500 °C зразки піддавали термічній обробці у дві стадії: за 1100 °C і за 1500 °C (протягом 70 год на повітрі). Фазовий склад отриманих зразків досліджували рентгенофазовим (DRON-3) та локальним рентгеноспектральним (Superprobe-733, JEOL, Японія, Пало-Альто, Каліфорнія) методами. У системі утворюються тверді розчини на основі різних поліморфних модифікацій вихідних оксидів та упорядкованих фаз типу перовскіту $LaLuO_3$ ($LaYbO_3$). Нових фаз у системі не знайдено. Побудовано ізотермічний перезріз діаграми стану системи La_2O_3–Lu_2O_3–Yb_2O_3 за 1500 °C. Встановлено, що в потрійній системі La_2O_3–Lu_2O_3–Yb_2O_3 утворюються поля твердих розчинів на основі гексагональної (A) модифікації La_2O_3, кубічної (C) модифікації Y_2O_3 і Lu_2O_3, а також упорядкованих фаз типу перовскіту $LaLuO_3$ і $LaYbO_3$ (R). Розраховано параметри елементарних комірок для твердих розчинів. У системі La_2O_3–Lu_2O_3–Yb_2O_3 за 1500 °C утворюється нескінченний ряд твердих розчинів на основі фази типу перовскіту. Максимальна розчинність Lu_2O_3 у R-фазі ~6 мол. % у перерізі Lu_2O_3 –(50 мол. % La_2O_3 – 50 мол. % Yb_2O_3). Область гомогенності R-фази простягається від 46 до 56 мол. % La_2O_3 у перерізі La_2O_3–(50 мол. % Lu_2O_3–50 мол. % Yb_2O_3).

Ключові слова: фазові рівноваги; оксиди лантану, лютецію, ітербію; параметри елементарної решітки.

**Corresponding author: e–mail: chudinovych_olia@ukr.net*

doi: 10.15421/jchemtech.v29i4.238943

Journal of Chemistry and Technologies, 2021, *29*(4), 485-494

ВЗАИМОДЕЙСТВИЕ ОКСИДОВ ЛАНТАНА, ЛЮТЕЦИЯ И ИТЕРБИЯ ПРИ ТЕМПЕРАТУРЕ 1500 °C

Ольга В. Чудинович[1,2], Александр И. Быков[1], Анатолий В. Самелюк[1]

[1]*Институт проблем материаловедения им. И.М. Францевича НАН Украины, г. Киев*

[2]*Национальный технический университет Украины "Киевский политехнический институт имени Игоря Сикорского", г. Киев*

Фазовые равновесия в тройной системе La_2O_3–Lu_2O_3–Yb_2O_3 при 1500 °C исследованы с помощью рентгенофазового анализа (РФА) и сканирующей электронной микроскопии во всем интервале концентраций. Исследуемые образцы разного состава готовили из растворов нитратов путем выпаривания, сушки и прокаливания при 800 °C. Для изучения фазовых равновесий при 1500 °C образцы подвергали термической обработке в две стадии: при 1100 °C и при 1500 °C (в течение 70 ч на воздухе). Фазовый состав полученных образцов исследовали рентгенофазовым (DRON-3) и локальным рентгеноспектральным (Superprobe-733, JEOL, Япония, Пало Альто, Калифорния) методами. В системе образуются твердые растворы на основе различных полиморфных модификаций исходных оксидов и упорядоченных фаз типа перовскита $LaLuO_3$ ($LaYbO_3$). Новые фазы в системе не найдены. Построен изотермический разрез диаграммы состояния системы La_2O_3–Lu_2O_3–Yb_2O_3 при 1500 °C. Установлено, что в тройной системе La_2O_3–Lu_2O_3–Yb_2O_3 образуются поля твердых растворов на основе гексагональной (A) модификации La_2O_3, кубической (C) модификации Y_2O_3 и Lu_2O_3, а также упорядоченных фаз типа перовскита $LaLuO_3$ и $LaYbO_3$ (R). Рассчитаны параметры элементарных ячеек для твердых растворов. В системе La_2O_3–Lu_2O_3–Yb_2O_3 при 1500 °C образуется бесконечный ряд твердых растворов на основе фазы типа перовскита. Максимальная растворимость Lu_2O_3 в R-фазе ~6 мол. % в сечении Lu_2O_3–(50 мол. % La_2O_3 – 50 мол. % Yb_2O_3). Область гомогенности R-фазы находится в пределах от 46 до 56 мол. % La_2O_3 в сечении La_2O_3–(50 мол. % Lu_2O_3–50 мол. % Yb_2O_3).

Ключевые слова: фазовые равновесия; оксиды лантана, лютеция, иттербия; параметры элементарной решетки.

Introduction

Oxides of rare earth elements (REE) due to the transparency in a wide spectral range, thermal and chemical stability, high absorption coefficient of X-rays are used to obtain fluorescent materials for a wide range of uses. Interest in optical ceramics as laser, scintillation media is due to high optical transparency in a wide range of wavelengths, thermal conductivity, good thermomechanical properties, radiation and chemical resistance and thermal stability. Ceramics has high manufacturability, wide possibilities of varying the chemical composition and can be obtained in the form of composite elements with different structures [1–5]. Doping lanthanum oxide with different REE allows obtaining substances with special optical, luminescent, dielectric properties, which makes it attractive as a material for photo converters. Ytterbium oxide has scintillation properties (fluorescence) and is used in optical fiber technology, as well as materials such as solar panels, lasers, radiation sources for portable X-ray sources. Materials based on REE oxide systems can be used to create high-temperature ceramics based on Si_3N_4 [9], in the optical industry [10], for dielectric films [11], and so on. The development of new materials and technologies for them needs phase equilibria studies and knowledge of properties of the phases formed in the systems.

Phase relations and structure of the phases formed in the La_2O_3-Yb_2O_3 system were studied in [12–15]. Using X-ray investigation of samples in the temperature range 1650-2000 °C, an ordered phase of perovskite $LaYbO_3$ (R) type has been revealed with a region of homogeneity of 38-55 mol % Yb_2O_3 [12]. The lattice periods for ordered lattice phase $LaYbO_3$ are: a = 0.601, b = 0.581, c = 0.839 nm, Z=4 [13]. According to [15], the $LaYbO_3$ crystallizes in two polymorphic modifications: orthorhombic and hexagonal with the transition temperature between them - 1850 °C. However, the polymorphism of the ordered phase is not confirmed yet [14; 15]. Accordingly to [15] the homogeneity field of R phase is 47-62 mol % Yb_2O_3 при 1400 °C, 45-63 mol % Yb_2O_3 at 1800 °C, 48–56 mol % Yb_2O_3 при 1500 °C [16]. It is assumed that the perovskite phase has a narrow homogeneity region. The maximum temperature of the R-phase existence is 2040 °C. Above this temperature, the X-Yb_2O_3 solid solutions exist in the concentration range from 0 to 91-92 mol % Yb_2O_3 [14]. These solid solutions are characterized by three-phase transitions: peritectic types and two eutectoid types near the compositions containing 28 mol % Yb_2O_3 at 1820 °C and 72 mol % Yb_2O_3 at 1930 °C, respectively.

In the system, there are solid solutions based on C-Yb_2O_3, low-temperature A, and high-temperature H of La_2O_3 modifications. The phase transition A ⇄ H has been determined using thermal analysis in the range of compositions with a high content of La_2O_3 (presence of exothermal pick on the cooling curves), though the solubility limits at the diagram of the binary system are not defined. The liquidus surface of the La_2O_3-Yb_2O_3 system is characterized by a minimum temperature point near the

composition containing 50 mol % Yb_2O_3 and transformation of perovskite-type.

At 1500 ºC in the La_2O_3-Yb_2O_3 system are formed solid solutions based on of hexagonal (A) modification of lanthanum oxide in the range of concentrations of 0–9 mol. % Yb_2O_3, cubic (C) modification of ytterbium oxide in the range of concentrations 98–100 mol. % Yb_2O_3, ordered phase of perovskite-type $LaYbO_3$ (R) in the range of concentrations 48–56 mol. % Yb_2O_3 [13]. The solubility of La_2O_3 in the C-type of Yb_2O_3 is ~ 2 mol. % at 1500 °C (50 h) [16]. The solubility of Yb_2O_3 in the A-type of La_2O_3 is ~ 9 mol. % at 1500 °C (50 h) [16].

Phase equilibria in the La_2O_3–Lu_2O_3 system were studied using X-ray and thermal analyzes at high temperatures [14]. Crystallization of the melt from a temperature above 2000 °C obtained single crystals of perovskite $LaLuO_3$. The lattice periods for ordered lattice phase $LaLuO_3$ are: a = 0.60, b = 0.579, c = 0.835 nm, the spatial group Pnam [14]. In [19] the calculation of oxygen vacancies in La_2O_3, Lu_2O_3, $LaLuO_3$ is given, the data on phase is not given. The region of solid solutions based on polymorphic modifications of La_2O_3 and Lu_2O_3 oxides has not been experimentally determined but has been calculated using the Thermo–Calc [19]. At 1500 ºC in the La_2O_3–Lu_2O_3 system are formed solid solutions based on hexagonal (A) modification of lanthanum oxide in the range of concentrations of 0–9 mol. % Lu_2O_3, cubic (C) modification of ytterbium oxide in the range of concentrations 96–100 mol. % Lu_2O_3, ordered phase of perovskite-type $LaLuO_3$ (R) in the range of concentrations 48–56 mol. % Lu_2O_3 [20]. The solubility of La_2O_3 in the C-type of Lu_2O_3 is ~4 mol. % at 1500 °C (50 h) [20]. The solubility of Lu_2O_3 in the A-type of La_2O_3 is ~ 9 mol. % at 1500 °C (50 h) [20].

State diagrams of the system based on the oxides of the end of a series of lanthanides are characterized by the formation of continuous series of solid solutions based on H– and C–modifications of REE oxides [21–25].

Experimental

Lanthanum oxide, La_2O_3 (LaO-1 grade), lutetium oxide, Lu_2O_3 (produced by Merck Corp.), ytterbium oxide, Yb_2O_3 (produced by Merck Corp.) (all 99.99 %), and analytical grade nitric acid were used as the starting materials. The lanthanum powder of preliminary dried at 200 °C for 2 h followed by dissolving in dilute nitric acid (1 : 1). The La_2O_3–Lu_2O_3–Yb_2O_3 test samples were prepared in concentration step 1–5 mol % from nitrate solutions with their subsequent evaporation and calcinations at 800 °C for 120 minutes. The prepared powders were subjected to single-action pressing in a steel die without a binder at 10–30 MPa to make pellets 5 mm in diameter and 4 mm in height.

Annealing at 1500 °C was conducted *via* two stages: first in a furnace with H23U5T (fecral) heaters at 1100 °C (for 200 h in air), then in a furnace with molybdenum disilicide heaters at 1500 °C (for 70 h in air). The test samples were heated at a rate of 3.5 °C/min. The samples were fired continuously.

The phase composition of the samples studied by X-ray diffraction (XRD, DRON-3), microstructural phase and electron microprobe X-ray (Superprobe-733, JEOL, Japan, Palo Alto, CA) analyses.

X-ray analysis of the test samples was performed by powder procedure on the apparatus DRON-3 at ambient temperature under the influence of Cu$K\alpha$ radiation. The scanning step was 0.05–0.1 degrees in the range 2θ = 15–90 °. The lattice parameters were calculated using the LATTIC code. The accuracy of the lattice parameter of the cubic phases was in the range of 0.0002 nm.

Microstructural studies were performed on polished sections and rough fractured surfaces of annealed samples in secondary electron (SE) and backscattered electron (BSE).

Results and discussion

Studies on solid phase interaction of La_2O_3 (A, hexagonal modification), Lu_2O_3 (C, cubic modification), and Yb_2O_3 (C, cubic modification) at temperatures of 1500 °C has shown that the La_2O_3–Lu_2O_3–Yb_2O_3 system consists of three types of solid solution, based on hexagonal modification (A-La_2O_3), cubic modification (C-Yb_2O_3(Lu_2O_3)), perovskite-type ordered phase R $LaLuO_3$($LaYbO_3$), separated by the two-phase fields (A+R) and (R+C) (Fig. 1).

The chemical and phase composition of the samples annealed at 1500 °C and lattice parameters of the equilibrium phases at the given temperature are shown in Table 1.

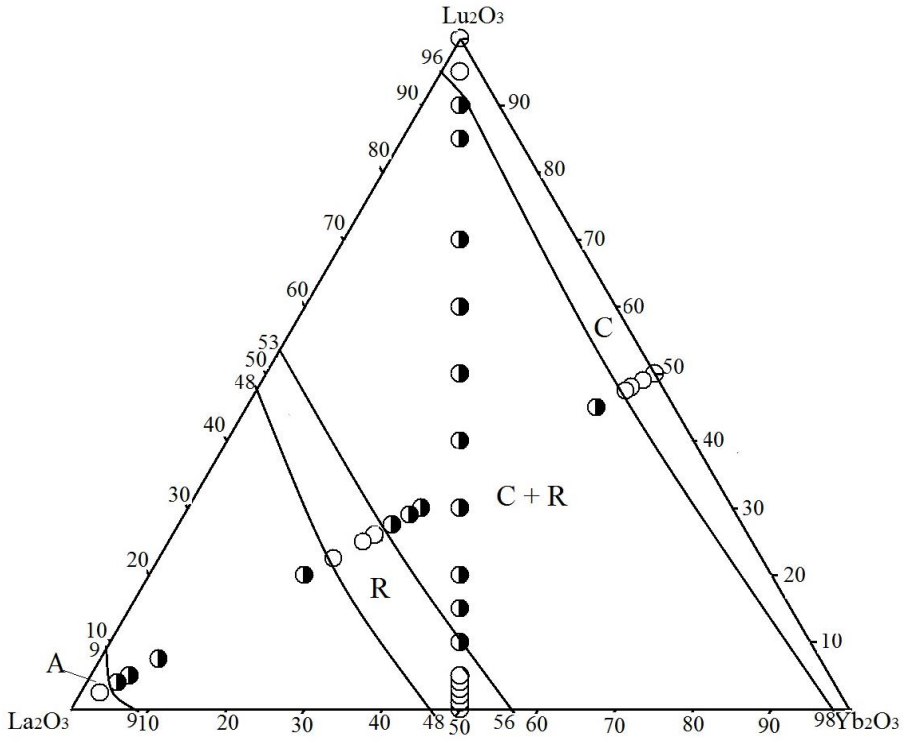

Fig. 1 Isothermal section for the system La_2O_3–Lu_2O_3–Yb_2O_3 at 1500 ºC (○ – single-phase samples, ◑ - two-phase samples)

Table 1

The chemical and phase compositions, lattice parameters of solid solutions, in the La_2O_3–Lu_2O_3–Yb_2O_3 system at 1500 °C, annealed for 70 h

Chemical composition (mol %)			Phase composition and lattice parameters of the phases	Lattice parameters of the phases $a \pm 0.0001$ (nm)			
Lu_2O_3	La_2O_3	Yb_2O_3		R			<C>
				a	*b*	*c*	*a*
Section Lu_2O_3—(50 mol. % La_2O_3—50 mol. % Yb_2O_3)							
0	50	50	R				
1	49.5	49.5	R	0.6020	0.5815	0.8290	—
2	49	49	R	0.6013	0.5824	0.8300	—
3	48.5	48.5	R	0.6013	0.5818	0.8310	—
4	48	48	R	0.6016	0.5826	0.8297	
5	47.5	47.5	R	0.6014	0.5819	0.8338	
10	45	45	R + <C>	0.6016	0.5817	0.8353	1.0419
15	42.5	42.5	R + <C>	0.6014	0.5819	0.8354	1.0418
20	40	40	R + <C>	0.6012	0.5801	0.8334	1.0413
30	35	35	R + <C>	0.6022	0.5828	0.8355	1.0430
40	30	30	R + <C>	0.6016	0.5826	0.8333	1.0416
50	25	25	R + <C>	0.6006	0.5816	0.8341	1.0404
60	20	20	R + <C>	0.5987	0.5817	0.8342	1.0403
70	15	15	R + <C>	0.5997	0.5822	0.8328	1.0403
85	7.5	7.5	R + <C>	0.5999	0.5827	0.8297	1.0404
90	5	5	R_{tr} + <C>				1.0403
95	2.5	2.5	<C>	—	—	—	1.0397
100	0	0	<C>	—	—	—	1.0390
Section La_2O_3—(50 mol. % Lu_2O_3—50 mol. % Yb_2O_3)							
50	0	50	<C>				1.0404

49	2	49	<C>				1.0405
48	4	48	<C>				1.0409
47.5	5	47.5	<C>				1.0409
45	10	45	R_{tr} + <C>				1.0412
30	40	30	R + <C>	0.6013	0.5801	0.8389	1.0412
29	42	29	R + <C>	0.5969	0.5835	0.8377	1.0415
27.5	45	27.5	R + <C>	0.5969	0.5828	0.8382	1.0418
26	48	26	R	0.5896	0.5810	0.8348	
25	50	25	R	0.5996	0.5822	0.8312	
22.5	55	22.5	R	0.5944	0.5856	0.8138	
20	60	20	<A>$_{tr}$ + R	0.6021	0.5851	0.8225	
7.5	85	7.5	<A> + R (a=0.6497,c=0.3825)	0.6020	0.5836	0.8214	
5	90	5	<A> + R_{tr} (a=0.6502,c=0.3828)				
4	92	4	<A> + R_{tr} (a=0.6511,c=0.3829)				
2.5	95	2.5	<A> (a=0.6507,c=0.3830)				

*Under given conditions (T= 1500 ºC, 70 h, in the air) the hexagonal A-La_2O_3 cannot be fixed, the hexagonal phase of A-$La(OH)_3$ is formed instead; <A> - solid solution based on hexagonal modification of La_2O_3; <C> - solid solution based on cubic modification of Lu_2O_3 and Yb_2O_3; R - solid solution based on perovskite-type ordered phases of $LaLuO_3$($LaYbO_3$); tr – traces.

The La_2O_3–Lu_2O_3–Yb_2O_3 system forms an infinite series of solid solutions based on the perovskite-type phase. The homogeneity range of the R-phase extends in compliance with its solubility limits in the boundary binary La_2O_3–Lu_2O_3 (48–56 mol. % Lu_2O_3) and La_2O_3–Yb_2O_3 (48–53 mol. % Yb_2O_3) systems. The maximum solubility of Lu_2O_3 in the R-phase is ~6 mol. % along section Lu_2O_3 – (50 mol. % La_2O_3 – 50 mol. % Yb_2O_3) (Fig. 2).

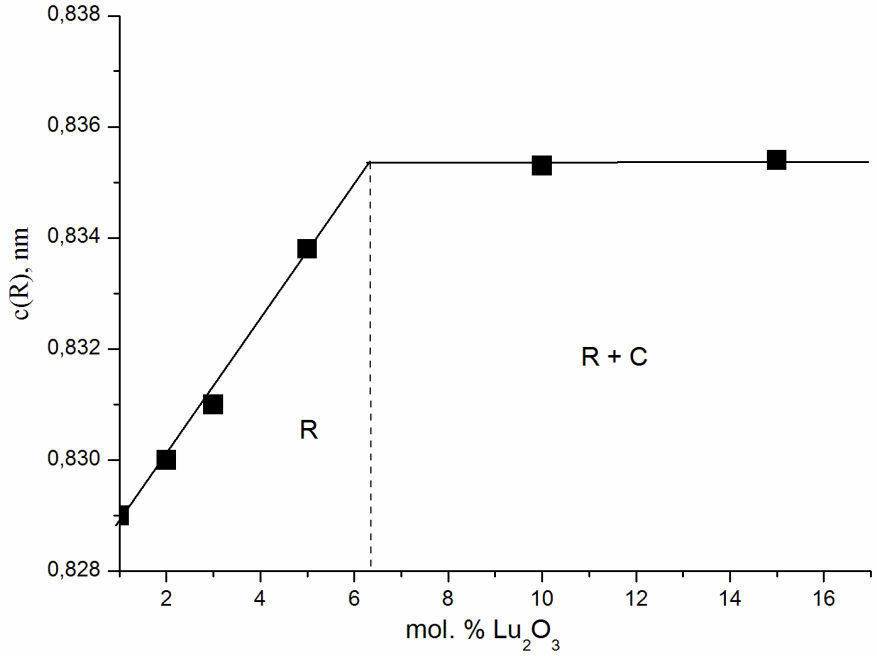

Fig. 2 Concentration dependence of lattice parameters (*c*) for solid solutions based on R-phase along the Lu_2O_3–(50 mol. % La_2O_3–50 mol. % Yb_2O_3) section in the system La_2O_3–Lu_2O_3–Yb_2O_3 at 1500 °C

The lattice parameters are changed from a = 0.6020 nm, b = 0.5815 nm, c = 0.8290 nm in single-phase sample, containing 49.5 mol % La_2O_3–1 mol % Lu_2O_3–49.5 mol % Yb_2O_3 to a = 0.6016 nm, b = 0.5817 nm, c = 0.8353 nm in two-phase sample (R + C), containing 45 mol % La_2O_3-10 mol % Lu_2O_3-40 mol % Yb_2O_3. The addition of the lutetium ion Lu^{3+} leads to its replacement of the yttrium ion Yb^{3+} (0.086 nm) in node B and increases the stability of the R-phase (increase in the conversion temperature).

The region of homogeneity of the R-phase extends from 46 to 56 mol. % La_2O_3 in the cross section La_2O_3– (50 mol.% Lu_2O_3–50 mol.% Yb_2O_3) (Fig. 3).

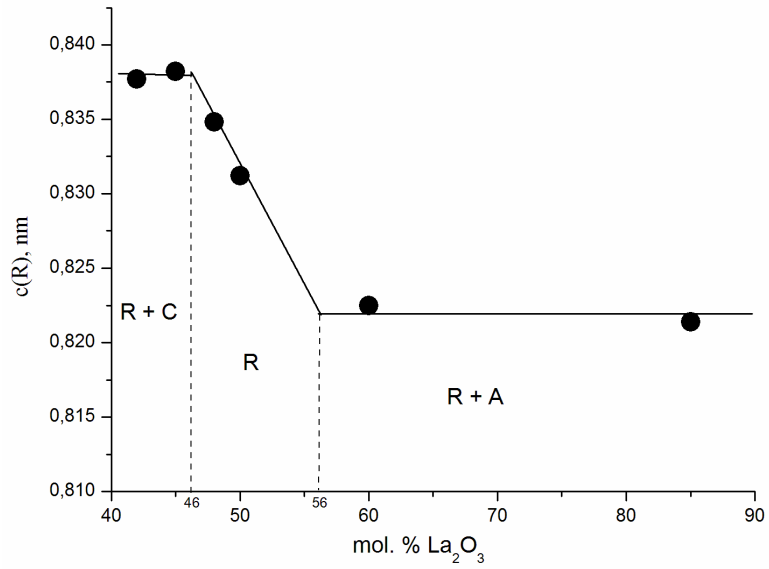

Fig. 3 Concentration dependence of lattice parameters (*c*) for solid solutions based on R-phase along the La_2O_3–(50 mol.% Lu_2O_3–50 mol.% Yb_2O_3) section in the system La_2O_3–Lu_2O_3–Yb_2O_3 at 1500 °C

Oxides of lutetium and ytterbium formed a continuous field of solid solutions based on the C-type of REE oxides. The region of the homogeneity of the solid solution is based on the cubic modification of lutetium and ytterbium oxides along the side of the Lu_2O_3 – Yb_2O_3 concentration triangle. The region of the homogeneity of the C-phase proceeds from the corresponding coordinates in the boundary binary systems La_2O_3–Lu_2O_3 (96–100 mol. % Lu_2O_3), La_2O_3–Yb_2O_3 (98–100 mol. % Yb_2O_3) i Lu_2O_3–Yb_2O_3 (0–100 mol. % Yb_2O_3). In this direction the region of the homogeneity of the C-phase indicates, however, that the substitution of Lu^{3+} ions by Yb^{3+} predominates, and vice versa. Using the concentration dependences of lattice parameters, it is established that the region of the homogeneity of the solid solutions based on C–Lu_2O_3 extends from 91 to 100 mol. % Lu_2O_3 along the section of Lu_2O_3–(50 mol. % La_2O_3–50 mol. % Yb_2O_3) (Fig. 4) and from 0 to 7 mol. % La_2O_3 along the section of La_2O_3–(50 mol. % Lu_2O_3–50 mol. % Yb_2O_3) (Fig. 5).

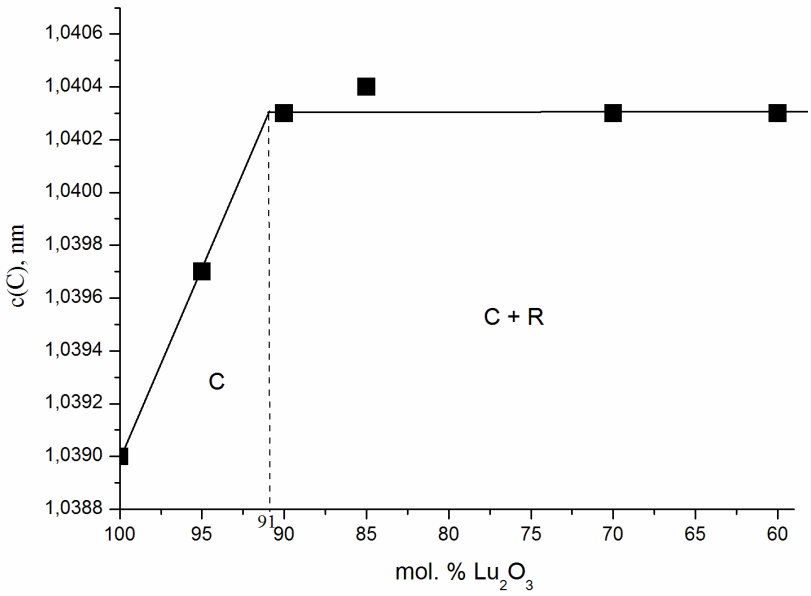

Fig. 4 Concentration dependence of lattice parameters (*c*) for solid solutions based on C-phase along the Lu_2O_3–(50 mol. % La_2O_3–50 mol. % Yb_2O_3) section in the system La_2O_3–Lu_2O_3–Yb_2O_3 at 1500 °C

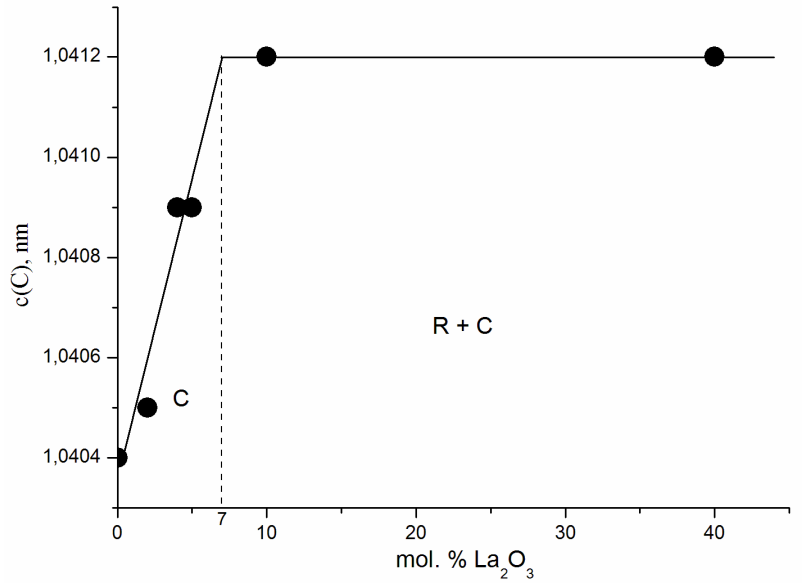

Fig. 5 Concentration dependence of lattice parameters (*c*) for solid solutions based on C-phase along the La_2O_3–(50 mol. % Lu_2O_3–50 mol. % Yb_2O_3) section in the system La_2O_3–Lu_2O_3–Yb_2O_3 at 1500 °C

Annealed samples with lanthanum oxide content from 55 to 100 mol. % in the air absorb moisture. For XRD data in these samples, instead of the hexagonal modification of La_2O_3, the hexagonal modification of A-$La(OH)_3$ is provided. The region of the homogeneity of the solid solution based on the hexagonal A-La_2O_3 modification is small. The region of this region of the homogeneity is concave in the direction of decreasing the content of ytterbium oxide and proceeds from the corresponding coordinates in the boundary binary systems La_2O_3–Lu_2O_3 (0–9 mol. %. Lu_2O_3) and La_2O_3–Yb_2O_3 (0–9 mol. % Yb_2O_3). Using the concentration dependences of lattice parameters, it is established that the region of the homogeneity of the solid solutions based on A-La_2O_3 extends from 94 to 100 mol. % La_2O_3 along the section of La_2O_3–(50 mol. % Lu_2O_3–50 mol. % Yb_2O_3) (Fig. 6).

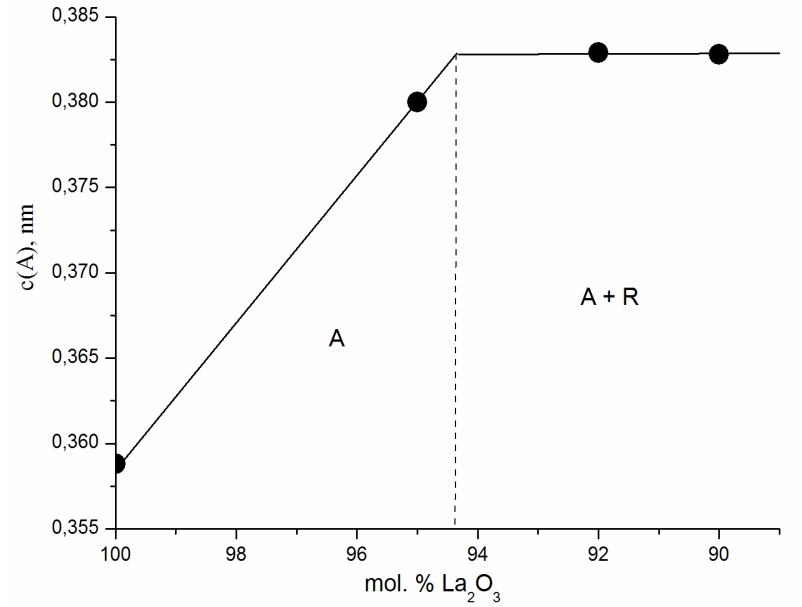

Fig. 6 Concentration dependence of lattice parameters (*c*) for solid solutions based on A-phase along the La_2O_3–(50 mol. % Lu_2O_3–50 mol. % Yb_2O_3) section in the system La_2O_3–Lu_2O_3–Yb_2O_3 at 1500 °C

The diffraction patterns of the samples characterizing the phase regions of the solid solutions in the La_2O_3–Lu_2O_3–Yb_2O_3 system at 1500 °C are shown in Fig. 7.

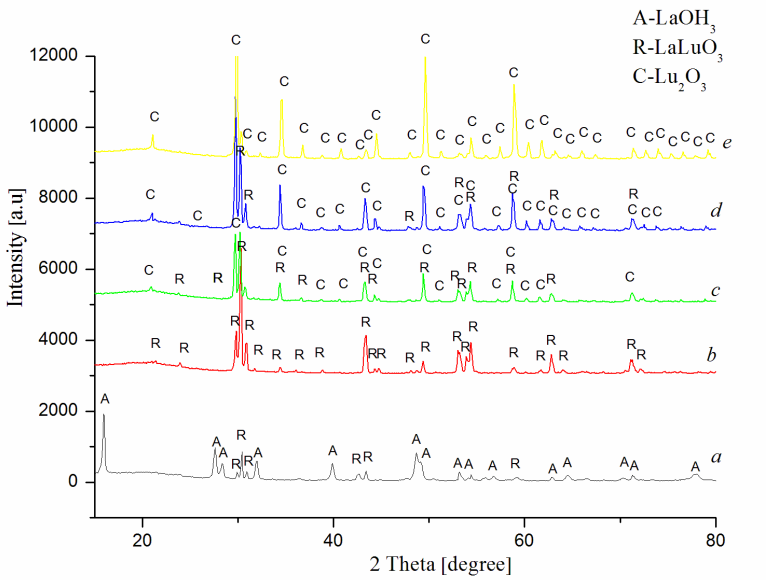

Fig. 7 XRD patterns of the samples from the La_2O_3–Lu_2O_3–Yb_2O_3 system heat-treated at 1500 °C: *a* – 92 mol % La_2O_3 – 4 mol % Lu_2O_3 – 4 mol % Yb_2O_3 (<A>+R); *b* – 49 mol % La_2O_3 – 2 mol % Lu_2O_3 – 49 mol % Yb_2O_3 (R); *c* – 35 mol % La_2O_3 – 30 mol % Lu_2O_3 – 35 mol % Yb_2O_3 (R+<C>); *d* – 30 mol % La_2O_3 – 40 mol % Lu_2O_3 – 30 mol % Yb_2O_3 (R+<C>); *e* – 2,5 mol % La_2O_3 – 95 mol % Lu_2O_3 – 2,5 mol % Yb_2O_3 (<C>)

The change in the microstructure of two-phase samples (C + R) depending on the concentration of lutetium oxide can be seen in Fig. 8. Fig. 8 is shown the microstructures of the samples along the section of Lu_2O_3–(50 mol. % La_2O_3–50 mol. % Yb_2O_3). The matrix light phase is the isotropic C phase. The matrix dark phase is the R-phase.

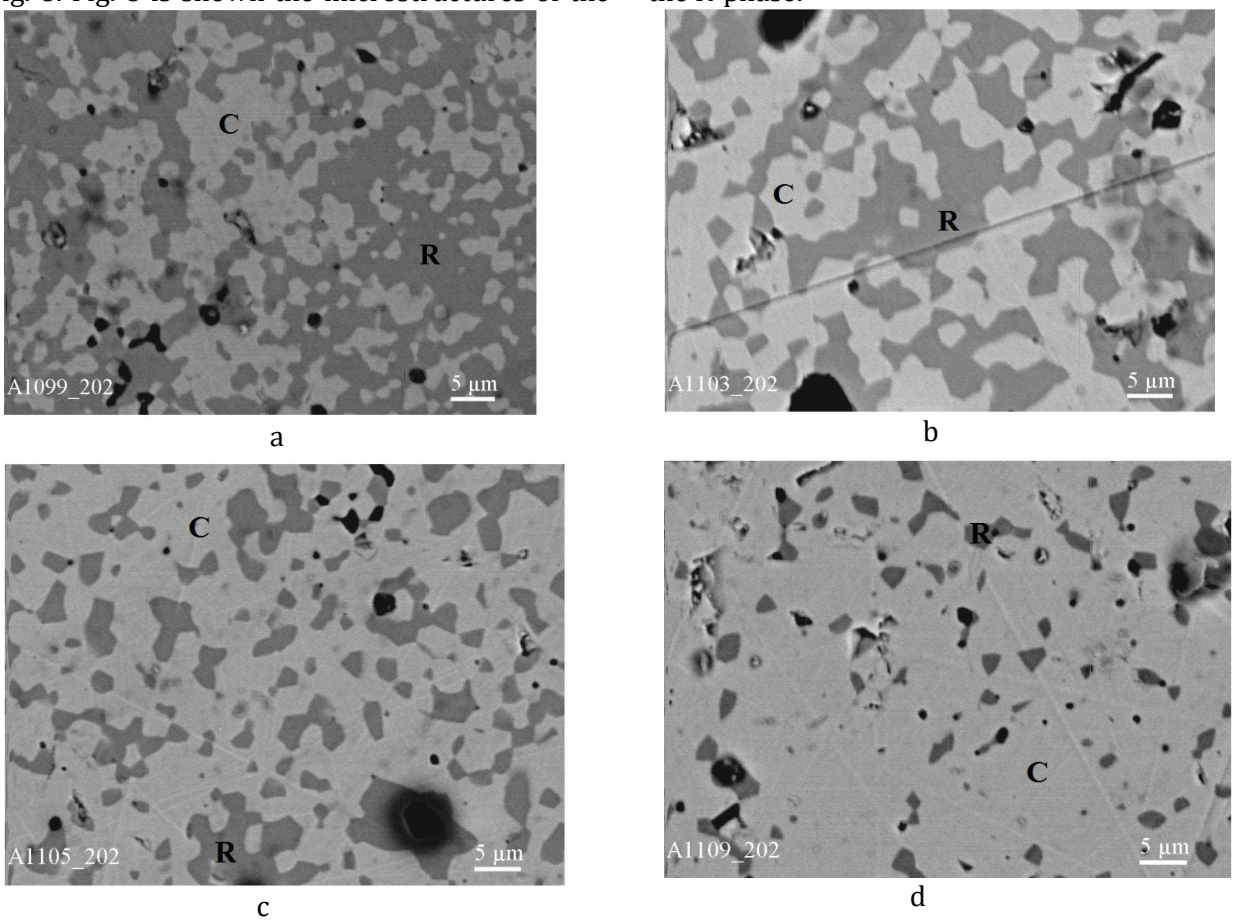

Fig. 8 SEM microstructures of the samples from the La_2O_3–Lu_2O_3–Yb_2O_3 system heat-treated at 1500 °C: a) 40 mol. % Lu_2O_3-30 mol. % La_2O_3-30 mol. % Yb_2O,BSE,×2000 (R+<C>);b) 60 mol. % Lu_2O_3-20 mol. % La_2O_3-20 mol. % Yb_2O,BSE, ×2000 (R+<C>;c) 70 mol. % Lu_2O_3-15 mol. % La_2O_3-15 mol. % Yb_2O,BSE,×2000 (R+<C>);d) 85 mol. % Lu_2O_3-7.5 mol. % La_2O_3-7.5 mol. % Yb_2O, BEI× 2000 BSE, ×2000 (R+<C>) (grey phase - <C>, dark phase – R, black – pores).

The ordering of the R-phase is a gradual diffusion-controlled process. In the early sintering stage, the samples acquire high relative density, and then the R phase becomes ordered in the dense ceramics. This leads to a great number of pores concentrated at grain boundaries of the C phase and the ordered R-phase.

Conclusions

The phase equilibria in the La_2O_3–Lu_2O_3–Yb_2O_3 system at 1500 °C were studied in the whole concentration range. The isothermal section has been developed. The solid solution of limited solubility based on all components in their different polymorphic modifications was found and characterized. The isothermal section of the La_2O_3–Lu_2O_3–Yb_2O_3 system at 1500 °C contains three one-phase fields (A-La_2O_3, R, C-Y_2O_3(Lu_2O_3)) and two two-phase fields (A + R) and (C + R).

Acknowledgements: This work was supported by G 5769 project.

Referens

[1] Wang, S.F., Zhang, J., Luo, D. W., Gu, F., Tang, D. Y., Dong, Z. L., Que, W. X., Zhang, T. S., Li, S., Kong, L.B. (2013). Transparent ceramics: Processing, materials and applications, *Prog. Solid State Chem., 41*, 20–54. http://dx.doi.org/10.1016/j.progsolidstchem.2012.12.002

[2] Sanghera, J., Bayya, S., Villalobos, G., Kim, W., Frantz, J., Shaw, B., Sadowski, B., Miklos, R., Baker, C., Hunt, M., Aggarwal, I., Kung, F. (2011). *Transparent ceramics for high-energy laser systems, Opt. Mater. 33*, 511–518. http://dx.doi.org/10.1016/j.optmat.2010.10.038

[3] Xie, W., Ivanov, M. G., Yavetskiy, R.P., Jiang, N., Shi, Y., Chen, Hao-Hong, Kou, H., Wang, J., Li, J. (2018). Eu:Lu_2O_3 transparent ceramics fabricated by vacuum sintering of co-precipitated nanopowders, Opt. Mater., 86, 550–561. https://doi.org/10.1016/j.optmat.2018.10.055

[4] Kryzhanovska, O.S., Baumer, V.N., Parkhomenko, S.V., Doroshenko, A.G., Yavetskiy, R.P., Balabanov, A.E., Tolmachev, A.V, Skorik, S.N., Li, J., Kuncser, A. (2019). Formation peculiarities and optical properties of highly-doped (Y0. 86LaO. 09YbO. 05) $2O_3$ transparent ceramics, *Ceram. Inter., 45*(13), 16002–16007. https://doi.org/10.1016/j.ceramint.2019.05.111

[5] Jun, A., Yoichi, S., Takunori, T., Akiyama, Ju. (2010). Laser ceramics with rare-earth-doped anisotropic materials, *Optics Lett. 35*(2), 3598–3600. http://dx.doi.org/10.1364/OL.35.003598

[6] Li, Sh., Zhu, X., Li, J., Yavetskiy, R. P., Ivanov, M. G., Liu, B., Liu, W., Pan, Yu. (2017). Fabrication of 5at. %Yb:$(La_{0.1}Y_{0.9})_2O_3$ transparent ceramics by chemical precipitation and vacuum sintering. *Opt. Mater. 71,* 56–61. http://dx.doi.org/10.1016/j.optmat.2016.06.017

[7] Zhuohao, X., Shijin, Yu., Li, Yu., Ruan, Sh., Ling Bing Kong, Huang, Q., Huang, Zh., Zhou, K., Su, H., Yao, Zh., Que, W., Liu, Y., Zhang, T., Wang, Ju., Liu, P., Shen, D., Allix, M., Zhang, J. Tang, D. (2020). Materials development and potential applications of transparent ceramics: A review, *Mater. S. Eng. 139*, 1–66. https://doi.org/10.1016/j.mser.2019.100518

[8] Permin, D.A., Balabanov, S.S., Novikova, A.V., Snetkov, I.L, Palashov, O.V., Sorokin, A.A., Ivanov, M.G. (2019). Fabrication of Yb-doped Lu_2O_3-Y_2O_3-La_2O_3 solid solutions transparent ceramics by self-propagating high-temperature synthesis and vacuum sintering, *Ceram. Inter. 45,* 522–529. https://doi.org/10.1016/j.ceramint.2018.09.204

[9] Urakami, R., Sato, Yu., Ogushi, M., Takeshi Nishiyama, Goto, K. A. Yamada, K., Teranishi, R., Kaneko, K., Mikito K. (2017). Phase transformation and interface segregation behavior in Si_3N_4 ceramics sintered with La_2O_3–Lu_2O_3 mixed additive, *J. Am. Cer. Soc., 100*(3), 1231–1240. http://dx.doi.org/10.1111/jace.14663

[10] Proessdorf, A., Niehle, M., Grosse, F., Rodenbach, P., Hanke, M., Trampert, M. (2016). Strain dynamics during La_2O_3/Lu_2O_3 superlattice and alloy formation, *J. Applied Phys., 119*, 215–301. https://doi.org/10.1063/1.4950875

[11] Tabata, T., Kita, K., Toriumi, A., Amorphous, High-k (2008). $LaLuO_3$ Dielectric Film for Ge MIS Gate Stack, *International Conference on Solid State Devices and Materials, Tsukuba*, 14-A-14, 14–15.

[12] Muller–Buschbaum Hk., Teske Chr. (1969). Kenntnis der Kristallstruktur von $LaYbO_3$, *J. Inorg. General. Chem., 369*(93–96), 255–264. https://10.1002/zaac.19693690316

[13] Muller–Buschbaum, Hk., Teske, Chr. (1969). Untersuchung des System La_2O_3–Yb_2O_3, *J. Inorg. General. Chem., 369*(3–6), 249–254. https://10.1002/ZAAC.19693690315

[14] Toropov, S.A. (1976). [*Diagrams of Refractory Oxide Systems*]. Nauka, Leningrad. (in Russian).

[15] Coutures, J., Sibieude, F., Foex, M. (1976). Etude a haute température des systèmes formés par les sesquioxydes de lanthane avec les sesquioxydes de lanthanides II. Influence de la trempe sur la nature des phases obtenues à la température ambiante, *J. Solid State Chem., 17*(4), 377–384. https:// 10.1016/S0022-4596(76)80006-0

[16] Chudinovych, O. V., Andrievskaya, E. R., Bogatyreva, Zh. D., Spasonova, L. M. (2016). [Interaction of lanthanum oxides and ytterbium at a temperature of 1500 °C]. *Sovr. Probl. Fiz. Materialoved., 25*, 15–28 (in Ukrainian).

[17] Coutures, J., Rouanet, A., Verges, R., Foex, M. (1976). Etude a haute temperature des systems formes par le sesquioxyde de lanthane et les sesquioxydes de lanthanides. I. Diagrammes de phases (1400 °C < *T* < *T* Liquide), *J. Solid State Chem., 17*(1–2), 172–182. http://dx.doi.org/10.1016/0022-4596(76)90218-8

[18] Traverse, J. P. (1971). Etude du Polymorphisme des sesquioxydes de terres rares, These, Grenoble.

[19] Xiong, K., Robertson, J. (2009). Electronic structure of oxygen vacancies in La_2O_3, Lu_2O_3 and $LaLuO_3$, *Microelectr. En., 86*(7-9), 1672–1675. https://doi.org/10.1016/j.mee.2009.03.016

[20] Chudinovych, O. V., Zhdanyuk, N.V., [Interaction of lanthanum oxides and lutetium at a temperature of 1500-1600 °C], *Ukrainian Chem. J., 86*(3) (2020) 19–25

(in Ukrainian). https://doi.org/10.33609/0041-6045.86.3.2020.19-25

[21] Andrievskaya, E. R. (2010). [Phase equilibria in the systems of hafnium, zirconium and yttrium oxides of rare earth elements], Naukova dumka, Kiev. (in Russian).

[22] Shannon, R. D. (1976). Revised effective ionic radii systematic studies of interatomic distances in halides and chalcogenides, *Acta Crystallogr. A. 32*(5), 751–754. https://doi.org/10.1107/S0567739476001551

[23] Zinkevich, M. (2007). Thermodynamics of rare earth sesguioxides, Prog. Mater. Sci., 52 597–647. https://doi.org/10.1016/j.pmatsci.2006.09.002

[24] Zinkevich, M., Thermodynamic Database for Rare Earth Sesquioxides, [(accessed on 16 April 2020)]; Available online: https://materialsdata.nist.gov/handle/11256/965.

[25] Pavlik, A., Ushakov, S.V., Navrotsky, A., Benmore, C. J., Weber, R.J.K. (2017). Structure and thermal expansion of Lu_2O_3 and Yb_2O_3 up to the melting points*, J. Nucl. Mater.,* 495, 385–391. https://doi.org/10.1016/j.jnucmat.2017.08.031